ELectronics EXpress

LETTER

IEICE Electronics Express, Vol.14, No.11, 1–11

An efficient blind calibration method for nonlinearity mismatches in *M*-channel TIADCs

Xiangyu Liu, Hui Xu, Husheng Liu, and Yinan Wang[a)]

College of Electronic Science and Engineering, National University of Defense Technology, No. 109, Deya Road, Changsha, Hunan 410073, China

a) *wangyinan@nudt.edu.cn*

Abstract: As gain, offset, and timing mismatches, nonlinearity mismatches also contribute to spurious components which deteriorate TIADC's performance. This paper proposes an efficient blind calibration method for nonlinearity mismatches in *M*-channel TIADCs. A modified model for nonlinearity mismatches is established by exploiting binary Hadamard transform (BHT) and differentiator. The calibration is composed of two stages—mismatches compensation and coefficients identification. The principle of mismatches compensation is to reconstruct estimations of the mismatches-induced spurious components and subtract them from the original TIADC's output. The coefficients identification is performed based on filtered-x least mean square (FxLMS) algorithm. By using improved model and calibration algorithm, the proposed method consumes less computational resource according to the complexity comparison. To tackle the 4-order nonlinearity mismatches in an 16-channel TIADC, the proposed method consumes 23% fewer multipliers than the previous work. Simulation results reveal that both effective resolution and dynamic range improve a lot after calibration.

Keywords: TIADC, frequency-dependent nonlinearity mismatches, binary Hadamard transform, filtered-x least mean square, differentiator

Classification: Circuits and modules for electronic instrumentation

References

[1] W. Black and D. Hodges: "Time interleaved converter arrays," IEEE Int. Solid-State Circuits Conf. (ISSCC) Dig. Tech. Papers (1980) 1022 (DOI: 10.1109/isscc.1980.1156111).

[2] K. Yang, *et al.*: "Timing skew calibration method for TIADC-based 20 GSPS digital storage oscilloscope," J. Circuits Syst. Comput. **25** (2016) 1650007 (DOI: 10.1142/S0218126616500079).

[3] S. Liu, *et al.*: "Adaptive semiblind background calibration of timing mismatches in a two-channel time-interleaved analog-to-digital converter," Analog Integr. Circuits Signal Process. **90** (2017) 1 (DOI: 10.1007/s10470-016-0839-5).

[4] P. Monsurro, *et al.*: "New models for the calibration of 4-channel time-interleaved ADCs using filter banks," IEEE Trans. Circuits Syst. II, Exp. Briefs

DOI: 10.1587/elex.14.20170468
Received May 3, 2017
Accepted May 15, 2017
Publicized May 26, 2017
Copyedited June 10, 2017

PP (2017) 1 (DOI: 10.1109/TCSII.2017.2662084).
[5] D. Prashanth and H.-S. Lee: "A sampling clock skew correction technique for time-interleaved SAR ADCs," 2016 Great Lakes Symp. VLSI (GLSVLSI) (2016) 129 (DOI: 10.1145/2902961.2903008).
[6] H. Chen, *et al.*: "An efficient digital calibration technique for timing mismatch in time-interleaved ADCs," IEICE Electron. Express **13** (2016) 20160524 (DOI: 10.1587/elex.13.20160524).
[7] H. Chen, *et al.*: "All-digital background calibration technique for timing mismatch of time-interleaved ADCs," Integration **57** (2017) 45 (DOI: 10.1016/j.vlsi.2016.11.003).
[8] X. Wang, *et al.*: "A novel autocorrelation-based timing mismatch calibration strategy in time-interleaved ADCs," 2016 IEEE Int. Symp. Circuits Syst. (ISCAS) (2016) 1490 (DOI: 10.1109/iscas.2016.7527540).
[9] S. Khan, *et al.*: "A fully digital background calibration technique for *M*-channel time-interleaved ADCs," Circuits Syst. Signal Process. **57** (2016) 1 (DOI: 10.1007/s00034-016-0456-7).
[10] R. Cimmino, *et al.*: "Blind and reference channel-based time interleaved ADC calibration schemes: A comparison," Proc. SPIE **9906** (2016) 990631 (DOI: 10.1117/12.2232969).
[11] H. Duc, *et al.*: "Estimation techniques for timing mismatch in time-interleaved analog-to-digital converters: Limitations and solutions," 2016 IEEE Int. Conf. Electron. Circuits Syst. (ICECS) (2016) 297 (DOI: 10.1109/icecs.2016.7841191).
[12] D. Li, *et al.*: "A background fast convergence algorithm for timing skew in time-interleaved ADCs," Microelectronics J. **47** (2016) 45 (DOI: 10.1016/j.mejo.2015.10.019).
[13] H. Mafi, *et al.*: "Digital blind background calibration of imperfections in time-interleaved ADCs," IEEE Trans. Circuits Syst. I, Reg. Papers **PP** (2017) 1 (DOI: 10.1109/tcsi.2017.2647758).
[14] Y. Wang, *et al.*: "Bandwidth-efficient calibration method for nonlinear errors in *M*-channel time-interleaved ADCs," Analog Integr. Circuits Signal Process. **86** (2016) 275 (DOI: 10.1007/s10470-015-0677-x).
[15] H. Liu, *et al.*: "A calibration method for nonlinear mismatches in *M*-channel time-interleaved analog-to-digital converters based on Hadamard sequences," Appl. Sci. **6** (2016) 362 (DOI: 10.3390/app6110362).
[16] P. Nikaeen and B. Murmann: "Digital compensation of dynamic acquisition errors at the front-end of high-performance A/D converters," IEEE J. Sel. Topics Signal Process. **3** (2009) 499 (DOI: 10.1109/JSTSP.2009.2020575).
[17] Y. Wang, *et al.*: "Joint blind calibration for mixed mismatches in two-channel time-interleaved ADCs," IEEE Trans. Circuits Syst. I, Reg. Papers **62** (2015) 1508 (DOI: 10.1109/TCSI.2015.2418835).
[18] Y. Wang, *et al.*: "Adaptive background estimation for static nonlinearity mismatches in two-channel TIADCs," IEEE Trans. Circuits Syst. II, Exp. Briefs **62** (2015) 226 (DOI: 10.1109/TCSII.2014.2368976).

1 Introduction

Analog-to-digital converter (ADC) plays an important role in modern electronic systems, such as radars, digital storage oscilloscopes, software defined radios, etc. Nevertheless, the sampling rate becomes a bottleneck due to the increasing instantaneous bandwidth of the measured signal. In order to accelerate the sampling

DOI: 10.1587/elex.14.20170468
Received May 3, 2017
Accepted May 15, 2017
Publicized May 26, 2017
Copyedited June 10, 2017

rate while maintaining the resolution, time-interleaved ADCs (TIADCs) are proposed in [1] and gaining momentum.

A TIADC is composed of M sub-ADCs. Every sub-ADC samples the input analog signal at an identical interval of MT_s in rotation, while the sampling instant of the next sub-ADC lags behind the previous one by a fixed interval of T_s. Ideally, when the output samples from all sub-ADCs are interleaved by phase, one can achieve an overall sampling interval of T_s. But in fact, there are always differences between the characteristics of sub-ADCs, namely mismatches, owing to variations in the manufacture. These mismatches will introduce spurious components in TIADC's output spectrum, which inevitably degrades the dynamic performance and effective resolution. Much emphasis has been put on the mitigation of linear mismatches, i.e., gain, offset, and timing mismatches [2, 3, 4, 5, 6, 7, 8, 9, 10, 11, 12, 13]. But there are only a few papers addressing the calibration of nonlinearity mismatches which are introduced due to the imperfection of analog front-end circuits as well as the differential and integral nonlinearities (DNL and INL) of sub-ADCs.

An adaptive blind calibration method for nonlinearity mismatches of M-channel TIADC was proposed in [14], however the influence of the input frequency on nonlinearity mismatches was not considered. Moreover, the error was reconstructed through output samples multiplied by the sinusoidal sequence, therefore occupying more computation resource. Then the method in [14] was improved by [15], where the error reconstruction was accomplished only by changing the sign of output samples, thus reducing the computational complexity. In broadband applications, the influence of input frequency on the mismatches parameters has to be considered. A model for frequency-dependent nonlinearity induced error of a single ADC was established by deploying differentiator and simplified Volterra series in [16]. Subsequently, an adaptive blind calibration method was proposed for frequency-dependent nonlinearity mismatches (FDNM) in two-channel TIADCs in [17]. Nonetheless, there is a lack of calibration method for FDNM in M-channel TIADCs.

This paper proposes an efficient blind calibration method for nonlinearity mismatches in M-channel TIADCs. The error model for single ADCs in [16] is first extended to M-channel TIADCs and then simplified using binary Hadamard transform (BHT). Filtered-x least mean square (FxLMS) algorithm is employed to identify the mismatches parameters. The imperfection is alleviated by removing the reconstructed error from output samples. The complexity comparison shows that the proposed method has less hardware consumption than [14]. For example, to calibrate 4-order nonlinearity mismatches in an 16-channel TIADC, the proposed method consumes 23% fewer multipliers than [14].

This paper is organised as follows. In Section 2, we propose the improved error model. The calibration algorithm is formulated in Section 3, while Section 4 presents the simulations to testify the performance. The computational complexity is compared in Section 5, and Section 6 concludes the paper.

DOI: 10.1587/elex.14.20170468
Received May 3, 2017
Accepted May 15, 2017
Publicized May 26, 2017
Copyedited June 10, 2017

2 Improved model using binary Hadamard transform

Fig. 1 illustrates the structure of a TIADC with nonlinearity mismatches and the timing diagram of its sampling process. The frequency-dependent nonlinearity is represented by transfer function $H_m(x, f)$.[1]

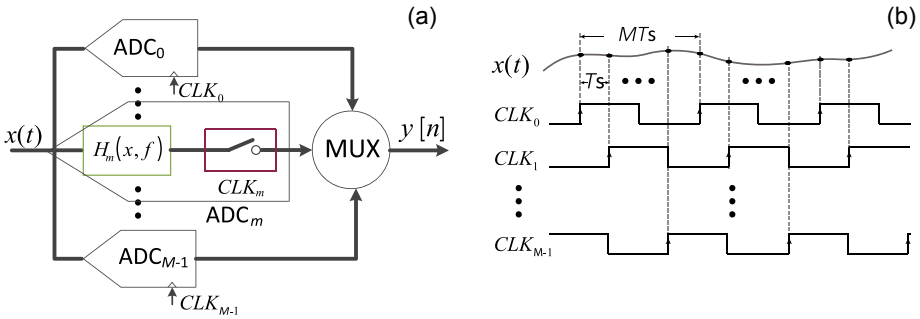

Fig. 1. (a) Structure of an M-channel TIADC with nonlinearity mismatches and (b) timing diagram of sampling process.

An analog signal $x(t)$ sampled at a period T_s generates the discrete-time sequence $x[n] = x(nT_s)$. The nonlinearity-induced error of an ADC can be modelled as [16]

$$e[n] = x_d[n] \sum_{l=2}^{L} a_l x^l[n], \tag{1}$$

where

$$x_d[n] = x[n] * h_d[n] \tag{2}$$

is the derivative of the input signal, and $h_d[n]$ is the unit impulse response of a differentiator; $x^l[n]$ stands for the l-th power of $x[n]$, while a_l is the nonlinearity coefficient. Moreover, the operator "$*$" denotes convolution.

In an M-channel TIADC scenario, the output sample is expressed as

$$y[n] = x[n] + e[n]. \tag{3}$$

The nonlinearity-mismatches-induced error is represented as

$$e[n] = x_d[n] \sum_{l=2}^{L} a_{n,l} x^l[n], \tag{4}$$

where $a_{n,l} = a_{n+M,l}$ is the nonlinearity coefficient of sub-ADCs. In a transformative view of Eq. (4), we might as well regard the overall error as a sum of errors generated by $L-1$ child-TIADCs working in parallel, while the l-th child-TIADC has only a nonlinearity level of $x^l[n]$. This equivalent architecture is shown in Fig. 2.

The discrete-time Fourier transform (DTFT) of $e[n]$ can be denoted as

$$E(e^{j\omega}) = X_d * \left[\sum_{l=2}^{L} (\vec{X}^l)^T \mathbf{W} \vec{a}_l \right], \tag{5}$$

where the frequency response of the differentiator is

[1]To concentrate on the nonlinearity mismatches, we assume other sorts of mismatches have already been calibrated.

DOI: 10.1587/elex.14.20170468
Received May 3, 2017
Accepted May 15, 2017
Publicized May 26, 2017
Copyedited June 10, 2017

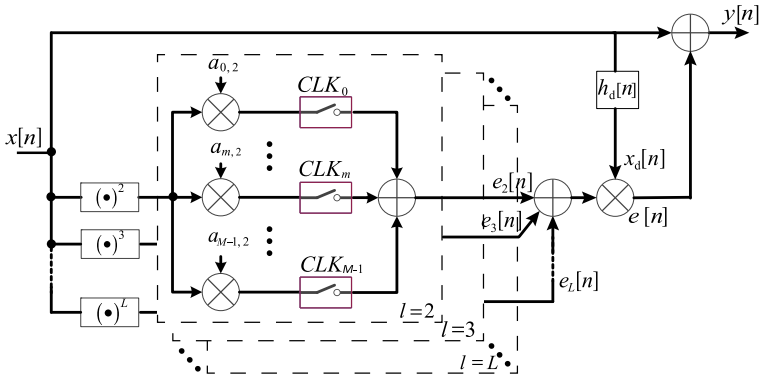

Fig. 2. Equivalent architecture of an M-channel TIADC with L-order nonlinearity mismatches.

$$X_{\mathrm{d}} = \mathrm{j}\omega X(\mathrm{j}\omega), \tag{6}$$

and the counterpart of $x^l[n]$ in frequency domain is

$$\vec{X}^l = \left[X^{*l}(\mathrm{j}\omega), X^{*l}\left(\mathrm{j}\left(\omega - \frac{2\pi}{M}\right)\right), \cdots, X^{*l}\left(\mathrm{j}\left(\omega - \frac{2(M-1)\pi}{M}\right)\right)\right]^{\mathrm{T}}, \tag{7}$$

$$X^{*l}(\mathrm{j}\omega) = \begin{cases} \dfrac{1}{2\pi}\displaystyle\int_{-\infty}^{\infty} X(\mathrm{j}\lambda)X(\mathrm{j}(\omega-\lambda))\mathrm{d}\lambda & l = 2 \\ (\underbrace{X * X * \cdots * X}_{(l-1)\text{ fold convolutions}})(\mathrm{j}\omega) & l > 2 \end{cases}, \tag{8}$$

while the discrete Fourier transform (DFT) matrix reads

$$\mathbf{W} = \frac{1}{M}\begin{bmatrix} 1 & 1 & \cdots & 1 \\ 1 & \mathrm{e}^{-\mathrm{j}\frac{2\pi}{M}} & \cdots & \mathrm{e}^{-\mathrm{j}\frac{2(M-1)\pi}{M}} \\ \vdots & \vdots & \ddots & \vdots \\ 1 & \mathrm{e}^{-\mathrm{j}\frac{2(M-1)\pi}{M}} & \cdots & \mathrm{e}^{-\mathrm{j}\frac{2(M-1)(M-1)\pi}{M}} \end{bmatrix}, \tag{9}$$

and the nonlinearity coefficients for the l-th child-TIADC in time domain is

$$\vec{a}_l = [a_{0,l}, a_{1,l}, \cdots, a_{M-1,l}]^{\mathrm{T}}. \tag{10}$$

For the purpose of developing a blind method, the model described in Fig. 2 should be further modified so that the coefficients to be estimated can be released from dependence on the time instant n. BHT can be used to achieve this goal. The binary Hadamard matrix exploited in this paper is defined as

$$\mathbf{F}_2 = \begin{bmatrix} 1 & 1 \\ 1 & -1 \end{bmatrix} \tag{11}$$

and

$$\mathbf{F}_{2m} = \begin{bmatrix} \mathbf{F}_m & \mathbf{F}_m \\ \mathbf{F}_m & -\mathbf{F}_m \end{bmatrix}.^{2} \tag{12}$$

Two properties of $\mathbf{F}_M$ will be used subsequently, which are $\mathbf{F}_M\mathbf{F}_M^{\mathrm{T}} = M\mathbf{I}$ and $\mathbf{F}_M = \mathbf{F}_M^{\mathrm{T}}$ with $\mathbf{I}$ being the identity matrix.

By applying BHT, Eq. (5) can be redeveloped as

[2] $m = 2^n$, and n is any positive integer.

DOI: 10.1587/elex.14.20170468
Received May 3, 2017
Accepted May 15, 2017
Publicized May 26, 2017
Copyedited June 10, 2017

$$E(e^{j\omega}) = X_d * \left[\sum_{l=2}^{L} (\vec{X}^l)^T \mathbf{W}\mathbf{F}_M \vec{c}_l\right], \tag{13}$$

where

$$\vec{c}_l = \frac{1}{M}\mathbf{F}_M \vec{a}_l \tag{14}$$

is the time-independent nonlinearity coefficient.

After the inverse discrete-time Fourier transform (IDTFT) of $E(e^{j\omega})$, we obtain a new expression of the error in time domain as

$$e[n] = x_d[n] \sum_{l=2}^{L} x^l[n] \sum_{k=0}^{M-1} T_k[n] c_{k,l}, \tag{15}$$

where $T_k[n]$ is the k-th row of $\mathbf{F}_M$ duplicated by $\lfloor \frac{n}{M} \rfloor$[3] times, and $c_{k,l}$ is the k-th element of the vector $\vec{c}_l$. The calibrated output sample is therefore

$$y_c[n] = y[n] - e[n]. \tag{16}$$

3 Calibration algorithm

Like many blind calibration approaches [14, 15, 18], it is also necessary to reserve an input-free mismatches band (IFMB) containing all the mismatches information except the input signal. Two conditions must be satisfied to acquire a proper IFMB — slight oversampling and wide enough input bandwidth. Most digital acquisition applications adopt slight oversampling to avoid spectral aliasing, which is not a demanding condition. The IFMB is often located around π rad/sample in the spectrum. The input signal's bandwidth B_i should therefore satisfy

$$\frac{\pi - B_h}{2} < B_i < \pi - B_h,^4 \tag{17}$$

where B_h is the width of IFMB and also the width of the highpass filter to be used in Section 3.2.

In this section, a structure for mismatches compensation is proposed, and then the adaptive estimation process is demonstrated.

3.1 Mismatches compensation structure

In practice, we cannot reconstruct the error as Eq. (15) even if the coefficients can be estimated quite precisely. This is because we are not capable of knowing the exact input sequence $x[n]$. One widely acceptable solution is approximating $x[n]$ by $y[n]$, which is true of a well-fabricated TIADC where the power of the error is much smaller than that of the input signal. Such being the case, the reconstructed error can be expressed as

$$\hat{e}[n] = y_d[n] \sum_{l=2}^{L} y^l[n] \sum_{k=0}^{M-1} T_k[n] \hat{c}_{k,l}, \tag{18}$$

where $\hat{c}_{k,l}$ is the estimate of $c_{k,l}$. So the compensated output sample is written as

[3]The operator "$\lfloor\cdot\rfloor$" means rounding down to the adjacent integer.

[4]The lower limit was illuminated in [14]. As for the upper limit, if $B_i > \pi - B_h$, the signal will reach the passband of the highpass filter, and the estimation process introduced in Section 3.2 will not converge.

DOI: 10.1587/elex.14.20170468
Received May 3, 2017
Accepted May 15, 2017
Publicized May 26, 2017
Copyedited June 10, 2017

$$y_c[n] \approx x[n] + y_d[n] \sum_{l=2}^{L} y^l[n] \sum_{k=0}^{M-1} T_k[n](c_{k,l} - \hat{c}_{k,l}). \tag{19}$$

The compensation structure is pictured in Fig. 3. The function of block "Opp" in Fig. 3(b) is to obtain the opposite number of the input. If $T_k[n] = 1$, the switch across "Opp" is on and "Opp" is bypassed; while if $T_k[n] = -1$, the switch is off and the opposite number of the input will be generated.

3.2 Adaptive coefficients estimation

FxLMS algorithm is used to adaptively identify $\hat{c}_{k,l}$. The cost function is selected as

$$\varepsilon[n] = y_c[n] * h_{hp}[n] = \sum_{l=2}^{L} \sum_{k=0}^{M-1} y_{l,k}^f[n](c_{k,l} - \hat{c}_{k,l}), \tag{20}$$

where $y_{l,k}^f[n] = y_d[n]y^l[n]T_k[n] * h_{hp}[n]$, and $h_{hp}[n]$ represents the unit impulse

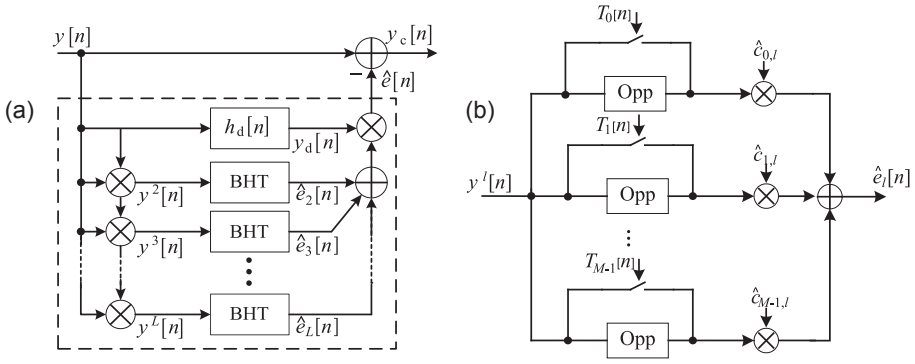

Fig. 3. (a) Compensation structure of an M-channel TIADC with L-order nonlinearity mismatches and (b) detailed BHT block.

response of a highpass filter. The width of the filter's passband is identical to that of IFMB. The coefficients are hence iterated as

$$\hat{c}_{k,l}[n+1] = \hat{c}_{k,l}[n] + \frac{\mu\varepsilon[n]y_{l,k}^f[n]}{\|y_{l,k}^f[n]\|^2 + \eta}, \tag{21}$$

where μ is the step size, η is the regularisation factor used to avoid the denominator being zero. Besides, the operator $\|\cdot\|$ stands for the Euclidean norm.

4 Simulation results

In this section, numerical simulations are performed to testify the performance of the proposed method via MATLAB®. In the following examples, we have some common settings. A 14-bit TIADC model will be employed. The step size μ is set as 0.5, and the regularisation factor η is 0.1. The highpass filter is implemented by a 62-order Type-I FIR filter with the stopband cutoff frequency of 0.8π rad/sample and the passband cutoff frequency of 0.95π rad/sample. The differentiator is implemented by a 40-order Type-I FIR filter with the same cutoff frequency as the highpass filter.

Example 1: A 4-channel TIADC model with 3-order nonlinearity mismatches

DOI: 10.1587/elex.14.20170468
Received May 3, 2017
Accepted May 15, 2017
Publicized May 26, 2017
Copyedited June 10, 2017

is used here. The 2nd and 3rd-order nonlinearity coefficients are set as

$$\vec{a}_2 = [0.01, -0.02, 0.007, -0.01]^{\mathrm{T}}, \tag{22}$$

and

$$\vec{a}_3 = [0.002, -0.005, -0.001, 0.004]^{\mathrm{T}} \tag{23}$$

respectively. A 7-tone sinusoidal signal is adopted as the input whose angular frequencies uniformly space from DC to 0.745π rad/sample.

The output spectra without and with calibration are demonstrated in Fig. 4. As can be seen from the figure, the spurious components induced by nonlinearity mismatches spread all over the entire band although the input signal is band-limited. The signal-to-noise-and-distortion ratio (SINAD) and spurious-free dynamic range (SFDR) before calibration are 41.51 dB and 41.75 dBc, while after calibration they are enhanced to 73.98 dB and 78.92 dBc respectively. It is noted that some spurious components still exist after calibration due to the difference between $x[n]$ and $y[n]$ (cf. Eq. (15) and (18)). They can be further suppressed by cascaded calibration described in [17], since $y[n]$ gets much closer to $x[n]$ after every calibration stage.

As mentioned in Eq. (14), the coefficients to be estimated are the BHT of $\vec{a}_{n,l}$ sets, namely $\vec{c}_{n,l}$. In this example, they are

$$\vec{c}_2 = [-0.00325, 0.01175, -0.00175, 0.00325]^{\mathrm{T}}, \tag{24}$$

and

$$\vec{c}_3 = [0, 0.0005, -0.0015, 0.003]^{\mathrm{T}} \tag{25}$$

respectively. The convergence results of the estimated coefficients are presented in Fig. 5. The coefficients converge to the preset values in no longer than 15000 sampling intervals.

Example 2: To further demonstrate the versatility of the proposed approach for more channels, an 8-channel TIADC model with 3-order nonlinearity mismatches is used here. The 2nd and 3rd-order nonlinearity coefficients are

$$\vec{a}_2 = [0.01, -0.02, 0.009, -0.005, -0.007, 0.008, 0.004, 0.02]^{\mathrm{T}}, \tag{26}$$

and

$$\vec{a}_3 = [0.001, -0.003, -0.002, 0, 0.001, -0.004, 0.002, 0.005]^{\mathrm{T}} \tag{27}$$

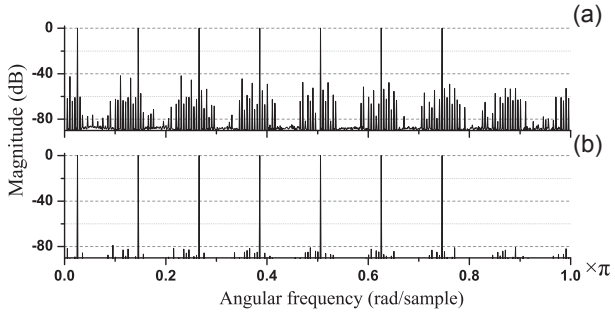

Fig. 4. Output spectra of a 4-channel TIADC with 3-order nonlinearity mismatches (a) before and (b) after calibration.

DOI: 10.1587/elex.14.20170468
Received May 3, 2017
Accepted May 15, 2017
Publicized May 26, 2017
Copyedited June 10, 2017

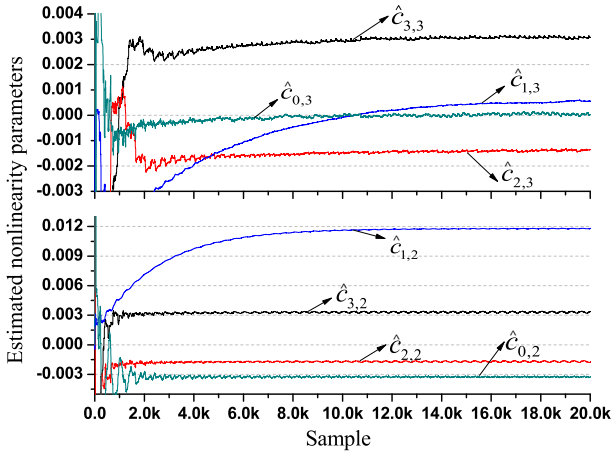

Fig. 5. Learning curves of the estimated coefficients for a 4-channel TIADC with 3-order nonlinearity mismatches.

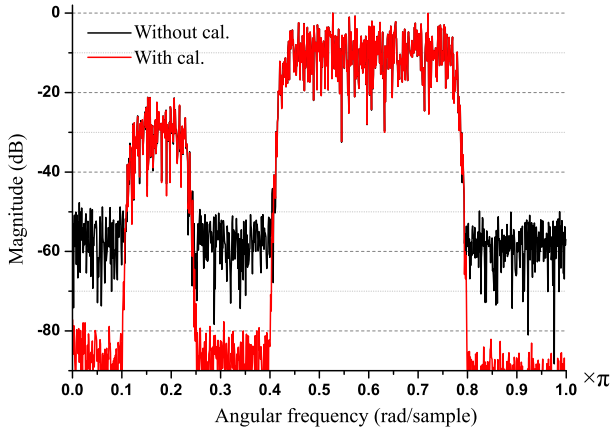

Fig. 6. Output spectra of an 8-channel TIADC with 3-order nonlinearity mismatches (a) before and (b) after calibration.

respectively. A dual-passband signal is employed as the input which is generated by passing a zero-mean white noise through a dual-passband filter. Fig. 6 depicts the output spectra without and with calibration. It is demonstrated that the magnitude of the error is reduced from approximately -50 dB to -80 dB after calibration.

Example 3: To verify the calibration effectiveness of the proposed method for higher order nonlinearity mismatches, a 4-channel TIADC model with 4-order nonlinearity mismatches is used here. The 2nd, 3rd and 4th-order nonlinearity coefficients are configured as

$$\vec{a}_2 = [0.01, -0.02, 0.007, -0.01]^{\mathrm{T}}, \tag{28}$$

$$\vec{a}_3 = [0.002, -0.005, -0.001, 0.004]^{\mathrm{T}}, \tag{29}$$

and

$$\vec{a}_4 = [0, -0.003, 0.002, 0.005]^{\mathrm{T}} \tag{30}$$

respectively. A 12-tone sinusoidal input is adopted whose angular frequencies uniformly space from 0.3π rad/sample to 0.63π rad/sample. The output spectra without and with calibration are depicted in Fig. 7. Before calibration the SINAD

DOI: 10.1587/elex.14.20170468
Received May 3, 2017
Accepted May 15, 2017
Publicized May 26, 2017
Copyedited June 10, 2017

and SFDR are 46.74 dB and 48.95 dBc, while they are enhanced to 74.78 dB and 78.92 dBc respectively after calibration.

5 Complexity comparison

A brief comparison among this work and previous research is presented in Table I.

The computational cost is manifest by the number of multipliers used for one sample's calibration which is divided into compensation stage followed by identification stage. It is worth noting that the multiplications between the operators used in both stages will be counted only in the compensation stage. Now that we

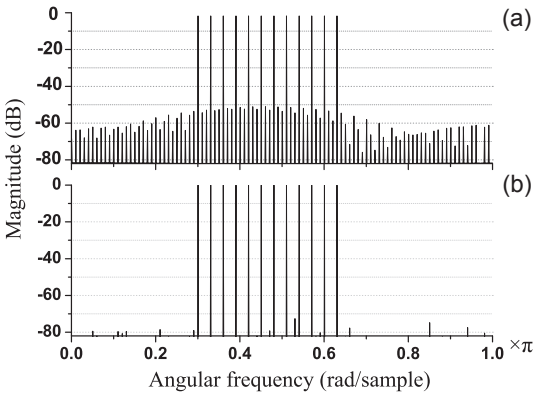

Fig. 7. Output spectra of a 4-channel TIADC with 4-order nonlinearity mismatches (a) before and (b) after calibration.

use FIR filters to implement the highpass filter and differentiator, the quantities of multipliers required for them are only $\frac{K_h}{2}+1$ and $\frac{K_d}{2}+1$ owing to the symmetric property of the coefficients.

When the channel number extends from 2 to M, the number of required multipliers in [14] increases by at least $2(M-1)(L-1)$, whereas the increment is only $(M-2)(L-1)$ in this paper for the compensation stage. As far as identification stage is concerned, the quantity of multipliers needed in [14] increases by at least $(M-2)(L-1)$, while it remains the same in this paper. That is because the output samples in [14] have to be multiplied by $\frac{2}{M}\cos(\frac{2\pi}{M}nk)$ and $\frac{2}{M}\sin(\frac{2\pi}{M}nk)$ separately. Nevertheless, only toggling the signs of the output samples is needed in this paper.

To give an intuitive impression, we adopt a 62-order Type-I FIR filter as the highpass filter, and a 40-order Type-I FIR filter as the differentiator. Fig. 8 shows the multipliers needed by the method in [14] and the proposed method in this paper. When $M=16$ and $L=4$, the proposed method consumes 23% fewer multipliers than [14].

Therefore, the proposed method has an advantage of low hardware consumption, and yet also imposes a restriction on the channel number to 2^n, which is however common in TIADCs and thus would cause little concern.

6 Conclusion

This paper introduces an efficient blind calibration method for nonlinearity mismatches in M-channel TIADCs. The error model for a single ADC is first extended

DOI: 10.1587/elex.14.20170468
Received May 3, 2017
Accepted May 15, 2017
Publicized May 26, 2017
Copyedited June 10, 2017

Table I. Comparison of different approaches

Method	[18]	[14]	[17]	This paper
Mismatches	FINM	FINM	FDNM	FDNM
Channel No.	2	M	2	$M = 2^n$
Compensation (mul./smpl.)	$3(L-1)$	M is even: $(2M+1)(L-1)$ M is odd: $(4M-1)(L-1)$	$K_d/2+1$ $+4(L-1)$	$K_d/2+1+$ $(M+2)(L-1)$
Identification (mul./smpl.)	$L(K_h/2+1)$ $+4(L-1)+1$	M is even: $L(K_h/2+1)+$ $(M+2)(L-1)$ $+1$ M is odd: $L(K_h/2+1)+$ $2(M+1)(L-1)$ $+1$	$L(K_h/2+1)$ $+4(L-1)+1$	$L(K_h/2+1)$ $+4(L-1)+1$

Note:
1) "mul./smpl." means the required multipliers for the calibration of one sample.
2) "K_h" is the order of the highpass filter.
3) "K_d" is the order of the differentiator.
4) "n" is any positive integer.
5) "FINM" stands for frequency-independent nonlinearity mismatches.

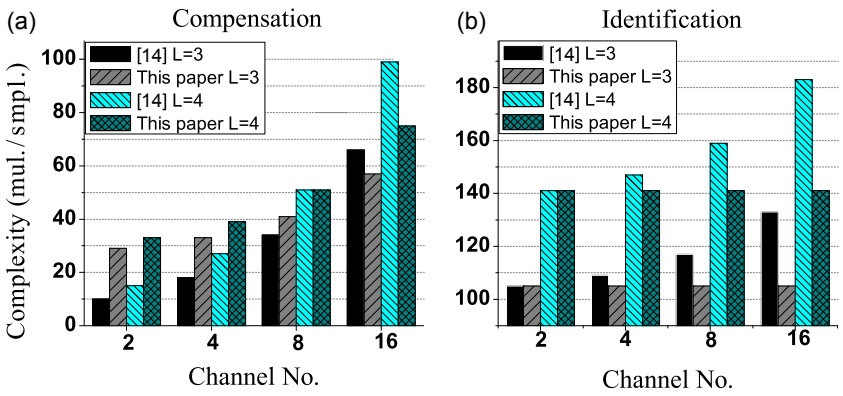

Fig. 8. Complexity comparison of (a) compensation stage and (b) identification stage.

to an M-channel TIADC and then simplified using BHT. Error reconstruction structure stemming from the model is elaborated and parameter identification based on FxLMS algorithm is presented. Simulations verify the recovery of effective resolution and the improvement of dynamic range. Complexity comparison reveals the economic virtue in the sense of resource consumption.

DOI: 10.1587/elex.14.20170468
Received May 3, 2017
Accepted May 15, 2017
Publicized May 26, 2017
Copyedited June 10, 2017